

# Assembly of the Inorganic Double Helix $\text{Mg}_6(\text{Et}_2\text{NCO}_2)_{12}$ by Fixation of Carbon Dioxide: Crystal and Solution Structure

M. Tyler Caudle,<sup>\*,†</sup> Ronald A. Nieman,<sup>†</sup> and Victor G. Young, Jr.<sup>‡</sup>

Department of Chemistry and Biochemistry, Arizona State University, Tempe, Arizona 85287-1604, and Department of Chemistry, University of Minnesota, Minneapolis, Minnesota 55455

Received August 16, 2000

The homoleptic magnesium carbamate complex  $\text{Mg}_6(\text{Et}_2\text{NCO}_2)_{12}$ , **1** ( $\text{Et}_2\text{NCO}_2^-$  = diethylcarbamato anion), was prepared by the reaction of dibutylmagnesium with diethylamine, followed by carboxylation using gaseous carbon dioxide. Crystallographic characterization demonstrated that **1** has the standard  $\text{M}_6(\text{R}_2\text{NCO}_2)_{12}$  structure and is a double helix of  $\text{MgO}_x$  ( $x = 5, 6$ ) coordination polyhedra with  $\Delta$  or  $\Lambda$  stereochemistry arising from the configuration around the six-coordinate  $\text{Mg}^{2+}$  cations. It crystallized in the orthorhombic space group  $Ccca$  with two molecules of  $\Delta\mathbf{1}$  and two of  $\Lambda\mathbf{1}$  per unit cell ( $a = 21.548 \text{ \AA}$ ,  $b = 25.094 \text{ \AA}$ ,  $c = 15.4485(11) \text{ \AA}$ ,  $\alpha = \beta = \gamma = 90^\circ$ ). Extensive solution characterization of **1** by 1-dimensional proton and  $^{13}\text{C}$  NMR spectroscopy and by two-dimensional  $^1\text{H}\{-^{13}\text{C}\}$  NMR correlation techniques verified that the helical structure is maintained in solution. Moreover, these measurements indicated that the intramolecular dynamics of **1** relating to motions of the ethyl groups was substantially hindered in solution. Correlation of the crystallographic and NMR structural studies indicated that this arises from a combination of hindered rotation about the carbamate C–N bond and efficient packing of the ethyl groups around the  $\text{Mg}_6\text{O}_{24}$  core. The result is an inverted-micelle-like structure for **1** in which the hydrophobic ethyl groups form a sheath largely restricting access to the hydrophilic  $\text{Mg}_6\text{O}_{24}$  core.

We recently prepared the first dinuclear carbamatomagnesium complex<sup>1</sup> and showed that its structure and intramolecular dynamics could be understood within the framework of the carboxylate shift structural paradigm.<sup>2</sup> The similarity of magnesium to divalent oxophilic transition metal ions prompted us to prepare a  $\text{Mg}^{2+}$  analogue for the iconic homoleptic carbamate complexes of formula  $\text{M}_6(\text{R}_2\text{NCO}_2)_{12}$  ( $\text{M} = \text{Mn, Fe, Co}$ ).<sup>3,4</sup> This would permit us to further explore the analogy between carboxylate and carbamate coordination chemistry in  $\text{Mg}^{2+}$  complexes. We show in this report that the  $\text{Mg}^{2+}$  analogue in this series is topologically isostructural with the transition metal derivatives, which spontaneously self-assemble from the reaction of anhydrous metal halides with secondary amines and carbon dioxide in a rudimentary example of synthetic  $\text{CO}_2$  fixation.

Detailed analysis of this new magnesium complex benefited from our ability to use high-resolution solution NMR as a complement to crystallographic structural studies. As a result, we have obtained new structural insight into the helical symmetry of  $\text{M}_6(\text{Et}_2\text{NCO}_2)_{12}$  complexes which consist of intertwined chains of metal coordination polyhedra whose structure is maintained in solution. The aggregation of intact ligands and metal ions into structures of higher order and complexity occasionally results in the spontaneous induction of helical symmetry,<sup>5,6</sup> but chemical principles leading to helical

symmetry from simple nonpolymeric ligands and metal ions are not well understood. We have therefore sought to reevaluate the solid and solution structure of the  $\text{M}_6(\text{Et}_2\text{NCO}_2)_{12}$  motif in terms of its helicity.

In this paper we report the crystal and solution structure of a homoleptic magnesium carbamate complex that we have identified as a coordination polyhedral double helix and show by NMR that the helical structure is maintained in solution. The structural and dynamic data indicate that the planarity of the  $\text{sp}^2$  nitrogen in the carbamate ligand and the partial double bond character in the C–N bond are critical features leading to conformational rigidity and helical symmetry in this molecule.

## Experimental Section

**Materials and Methods.** Diethylamine, dibutylmagnesium, and anhydrous magnesium bromide were obtained from Aldrich. Diethylamine was distilled from potassium hydroxide prior to use. *n*-Hexane, *n*-heptane, and chloroform-*d* were distilled from calcium hydride and stored under nitrogen. All synthetic and analytical manipulations were performed under a nitrogen atmosphere either in a Vacuum Atmospheres drybox or in standard Schlenk glassware. All precautions were maintained to prevent exposure to water. Proton and  $^{13}\text{C}$  NMR spectra were measured in on a Varian INOVA 500 instrument at ambient temperature.

\* To whom correspondence should be addressed.

<sup>†</sup> Arizona State University.

<sup>‡</sup> University of Minnesota.

- (1) Caudle, M. T.; Kampf, J. W. *Inorg. Chem.* **1999**.
- (2) Rardin, L.; Tolman, W. B.; Lippard, S. J. *New. J. Chem.* **1991**, *15*, 417–430.
- (3) Belli-Dell'Amico, D.; Calderazzo, F.; Giovannitti, B.; Pelizzi, G. *J. Chem. Soc., Dalton Trans.* **1984**, 647–652. Belli-Dell'Amico, D.; Calderazzo, F.; Labella, L.; Maichle-Mössner, C. *J. Chem. Soc., Chem. Commun.* **1994**, 1555–1556.
- (4) Belforte, A.; Calderazzo, F.; Zanazzi, P. F. *J. Chem. Soc., Dalton Trans.* **1988**, 2921–2927.

- (5) Li, D.-G.; Liu, C.-M.; You, X.-Z.; Fu, W.-Q.; Chen, W.; Lo, K. M. *J. Coord. Chem.* **1998**, *46*, 33–41. Polcar, C.; Lambert, F.; Cesario, M.; Morgenstern-Badarau, I. *Eur. J. Inorg. Chem.* **1999**, 2201–2207. Gier, T.; Bu, X.; Feng, P.; Stucky, G. D. *Nature* **1998**, *395*, 154–157. Soghomonian, V.; Chen, Q.; Haushalter, R. C.; Zubieta, J.; O'Connor, C. J. *Science* **1993**, *259*, 1596–1599.
- (6) Williams, A. *Chem.—Eur. J.* **1997**, *3*, 15–19. Constable, E. C. In *Comprehensive Supramolecular Chemistry*; Sauvage, J.-P., Hosseini, M. W., Eds.; Elsevier: Oxford, 1996; Vol. 9, pp 213–252. Lehn, J. M.; Rigault, A.; Siegel, J.; Harrowfield, J.; Chevrier, B.; Moras, D. *Proc. Natl. Acad. Sci. U.S.A.* **1987**, *84*, 2565–2569.

**Table 1.** Crystallographic Data

formula	$C_{15}H_{30}Mg_{1.5}N_3O_6$
fw	384.89
color	clear
crystal system	orthorhombic
space group	<i>Ccca</i>
	$a = 21.548(2) \text{ \AA}$
	$b = 25.094(2) \text{ \AA}$
	$c = 15.4485(11) \text{ \AA}$
	$\alpha = \beta = \gamma = 90^\circ$
<i>V</i>	$8353.5(1) \text{ \AA}^3$
<i>Z</i>	16
$\lambda$	$0.71073 \text{ \AA}$
temp	173(2) K
<i>R</i> indices ( $I > 2\sigma(I) = 3945$ ) <sup>a</sup>	0.0323
<i>R</i> indices (all data) <sup>a</sup>	0.0434
goodness-of-fit on $F^2$	1.045

<sup>a</sup> 4797 data points, 253 parameters, 63 restraints.

**Synthesis of  $Mg_6(Et_2NCO_2)_{12}$ .** Diethylamine (20 mmol) was dissolved in 70 mL of anhydrous *n*-hexane. A solution containing 10 mmol dibutylmagnesium (1.0 M in *n*-heptane) was added to the diethylamine solution dropwise under nitrogen with vigorous stirring, yielding a white precipitate after 30 min (note: dibutylmagnesium is potentially pyrophoric and reacts violently with small amounts of water). This slurry was exposed to anhydrous carbon dioxide gas. The reaction is exothermic, and precautions were taken to prevent overheating of the solution. After nearly all solid had dissolved, the solution was filtered through a pad of Celite under nitrogen, and the clear solution evaporated under a slow stream of nitrogen to give 1.7 g (66%) of  $Mg_6(Et_2NCO_2)_{12}$ , **1**. X-ray quality crystals of this complex were obtained by slow evaporation of a solution of **1** in *n*-hexane under nitrogen. Compositional analysis, % found(% calcd): C, 46.9(46.9); H, 7.6(7.8); N, 10.8(10.9). IR ( $cm^{-1}$ ): 1620 (asymm  $-CO_2$ ); 1492 (symm  $-CO_2$ ); 807 ( $-CO_2$  bending).

For an alternate preparation of **1**, 1.5 g (8.15 mmol) of  $MgBr_2$  and 3.4 mL (32.6 mmol) of diethylamine were combined in 50 mL of *n*-hexane and exposed to anhydrous  $CO_2$  gas. After 24 h, solid diethylammonium bromide was removed by filtration and the filtrate evaporated to dryness. The resulting off-white residue was dissolved in 50 mL *n*-heptane, filtered, and evaporated under reduced pressure to give 1.48 g (71%) of white crystalline solid **1**. IR and NMR analysis showed that this material was identical to **1** prepared by the method above.

#### Single-Crystal X-ray Data Collection and Structure Refinement.

A crystal of **1** was attached to a glass fiber and mounted on a Siemens SMART system for data collection at 173(2) K. Final cell constants were calculated from a set of 8192 strong reflections from the actual data collection. The space group *Ccca* was determined based on systematic absences and intensity statistics.<sup>7</sup> A successful direct-methods solution was calculated which provided most non-hydrogen atoms from the E-map. Several full-matrix least-squares/difference Fourier cycles were performed which located the remainder of the non-hydrogen atoms. All non-hydrogen atoms were refined with anisotropic displacement parameters. All hydrogen atoms were placed in ideal positions and refined as riding atoms with relative isotropic displacement parameters. One ethyl group was disordered in a 0.75/0.25 ratio. The disorder was severe enough to employ SHELXTL SAME restraints. Disordered atoms C8 and C8' were constrained to have the same  $U_{ij}$  displacements. Refer to Table 1 for additional crystal and refinement information.

## Results

Complex **1** can be prepared by the condensation of diethylamine and carbon dioxide in the presence of magnesium bromide. However, we found it synthetically more convenient to react dibutylmagnesium with diethylamine to give the

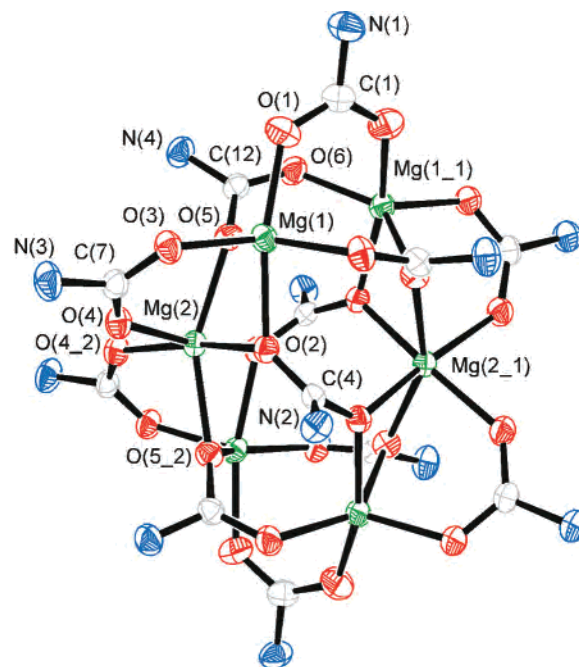


**Figure 1.** ORTEP drawing of **1** showing atomic positions in the  $Mg_6$  core. Ethyl groups have been omitted for clarity. Only relevant symmetry related atoms are labeled. Bond lengths ( $\text{\AA}$ ):  $Mg1-O1$ , 1.987(11);  $Mg1-O2$ , 2.089(10);  $Mg1-O3$ , 1.9632(9);  $Mg1-O5$ , 2.047(10);  $Mg1-O6_1$ , 2.0124(10);  $Mg2-O4$ , 2.0312(9);  $Mg2-O2$ , 2.0910(9);  $Mg2-O5$ , 2.1426(9);  $Mg1 \cdots Mg1_1$ , 3.39;  $Mg1 \cdots Mg2$ , 3.13;  $Mg2 \cdots Mg2_1$ , 4.42. Bond angles (deg):  $O3-Mg1-O6_1$ , 121.59(4);  $O5-Mg2-O3$ , 98.72(4);  $O5-Mg1-O6_1$ , 137.99(4);  $O1-Mg1-O2$ , 163.15(4);  $O4-Mg2-O2$ , 84.97(3);  $O4-Mg2-O4_1$ , 86.79(5);  $O5-Mg2-O5_1$ , 154.66(5).

magnesium amido intermediate of composition  $Mg(NEt_2)_2$  in situ. Exposure of this solution to anhydrous carbon dioxide gas resulted in formation of the magnesium carbamate complex, a reaction with precedent in several oligomeric magnesium amido species.<sup>8,9</sup> These reactions can formally be considered to arise from addition of the  $Mg-N$  unit across the unsaturated  $C=O$  bond in  $CO_2$ . The alternative reaction used magnesium bromide as the  $Mg^{2+}$  source, reacting it with diethylamine and carbon dioxide in a one-pot preparation yielding **1**. This alternative reaction is directly analogous to that used by Calderazzo et al. in the preparation of the transition metal derivatives.<sup>3,4</sup> A metathesis method was previously employed in the preparation of the compositionally related complex  $Mg(i\text{-}pr_2NCO_2)_2$ ,<sup>10</sup> which was not structurally characterized.

Details of the crystallographic data collection and refinement are presented in Table 1.<sup>8</sup> The hexanuclear molecular unit contains six magnesium ions supported by twelve diethylcarbamate ligands as shown in the ORTEP diagram in Figure 1. When represented in terms of linked coordination polyhedra for the six magnesium ions, Figure 2, we see that the molecule may be topologically regarded as two trinuclear  $Mg_3O_{12}$  chains cross-linked by diethylcarbamate ligands and related to each other by a molecular  $C_2$  axis of rotation. Each chain is composed of three edge-shared  $MgO_x$  ( $x = 5, 6$ ) polyhedra. The central magnesium ion has six-coordinate pseudooctahedral coordina-

- (8) An ORTEP of **1** without accompanying preparative or structural data was reported by: Chang, C.-C.; Ameerunisha, M. S. *Coord. Chem. Rev.* **1999**, *189*, 199–278.
- (9) Sanchez, R.; Felan, O. *Main Group Met. Chem.* **1995**, *18*, 225–231. Ruben, M.; Walther, D.; Knake, R.; Görls, H. *Eur. J. Inorg. Chem.* **2000**, 1055–1060.
- (10) Calderazzo, F.; Pampaloni, G.; Sperrle, M.; Englert, U. *Z. Naturforsch.* **1992**, *47*, 389–394.

(7) SHELXTL-Plus V5.0; Siemens Industrial Automation, Inc.: Madison, WI.

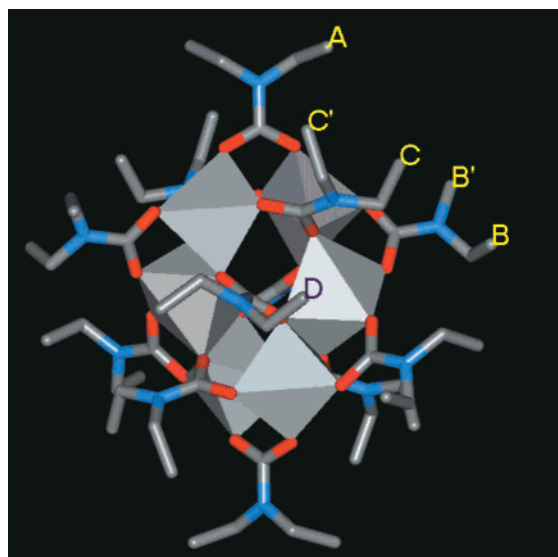


**Figure 2.** Structure of **1** showing magnesium coordination polyhedra in light gray and oxygen atoms in red. A–D indicate inequivalent ligands. Prime marks indicate inequivalent ethyl groups. Symmetry-related ligands are not labeled.

tion geometry and is linked via two edges to the basal planes of two symmetry-equivalent terminal magnesium ions having five-coordinate distorted square pyramidal geometry. Because the two shared edges are disposed as the blades of a propeller, individual chains possess either  $\Delta$  or  $\Lambda$  stereochemistry imparted by the stereochemistry of the central magnesium ion. Two chains of complementary stereochemistry are intertwined about the molecular  $C_2$  axis to form a double helix of coordination polyhedra, making **1** a rare example of an inorganic double helix arising directly from chains of inorganic coordination polyhedra. Of the four individual molecules of **1** in the unit cell, two have  $\Delta$  helical configuration and two have  $\Lambda$  configuration, making the crystal a racemic mixture of stereoisomers.

In **1**, Mg–O linkages to a terminal carbamate oxygen have an average bond length of 2.00(3) Å and those to a bridging carbamate oxygen have a predictably longer average bond length of 2.09(4) Å. While **1** is topologically identical to the corresponding  $d^5$   $Mn^{2+}$  derivative,<sup>4</sup> all Mg–O bond lengths are approximately 0.10 Å shorter, reflecting the relative five- and six-coordinate ionic radii of  $Mg^{2+}$  (80 pm, 86 pm) and  $Mn^{2+}$  (89 pm, 97 pm).<sup>11</sup> The interhelical  $Mg(1)\cdots Mg(1_2)$  vector is bridged by three carbamate ligands in a  $\mu_{1,3}$  mode and has a distance is 3.39 Å. The  $Mg(1)\cdots Mg(2)$  vector is spanned by two  $\mu_{1,1}$  carbamate ligands and one  $\mu_{1,3}$  ligand and is predictably shorter, 3.13 Å.

The characteristic molecular symmetry of **1** consists of three mutually perpendicular  $C_2$  axes of rotation. This gives four symmetry-inequivalent diethylcarbamato ligands in this complex, corresponding to the carboxyl carbon nuclei C1, C4, C7, and C12. Carbons C1 and C4 lie on a  $C_2$  axis, and so there are two of each. On the other hand, nuclei C7 and C12 do not lie on a  $C_2$  axis and there are four of each of these. The 500 MHz  $^{13}C$  NMR spectrum in  $CDCl_3$ , Figure 3, resolves four signals in the carboxyl region at 162.25, 162.38, 162.74, and 162.90 ppm with respective relative intensities of 1:2:1:2. This agreement between the number and intensities of symmetry-predicted carbon signals and the experimentally observed  $^{13}C$  NMR spectrum provides preliminary evidence that the hexanuclear helical architecture prevails in solution as well as in the solid state.

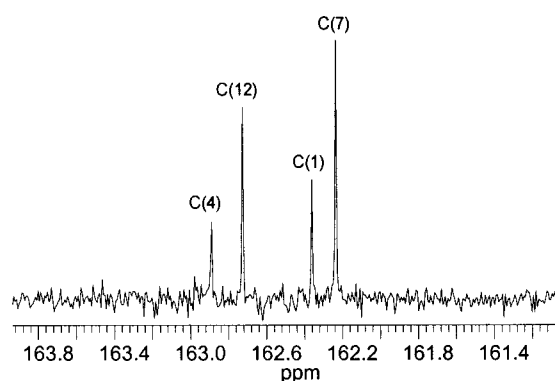


**Figure 3.**  $^{13}C$  NMR spectrum of **1** in the carboxyl region, showing assignment of the carboxyl carbon atoms. Assignments were made based on intensity ratios and 2D  $^1H$ – $^{13}C$  correlation data.

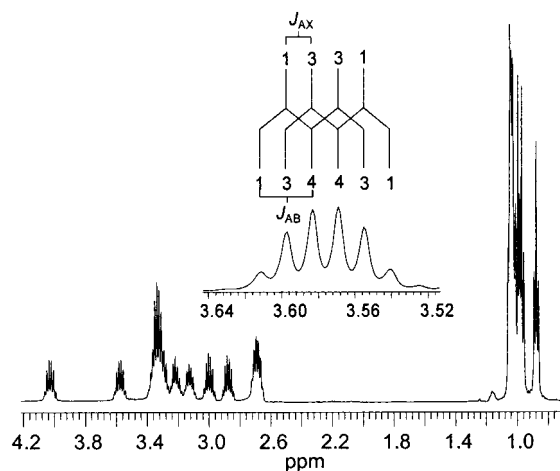
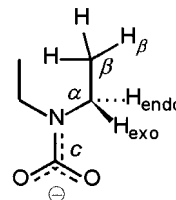


**Figure 4.** Proton NMR spectrum of **1** in  $CDCl_3$ . Inset shows an expansion of the methylene region. See Table S1<sup>12</sup> for assignments based on 2D  $^1H$ – $^{13}C$  correlation data.

Two of the four symmetry-inequivalent diethylcarbamato ligands lie away from  $C_2$  axes, which makes their ethyl groups inequivalent. The result is six symmetry-inequivalent ethyl groups. Furthermore, the helical axis makes the two methylene protons within a single ethyl group symmetry-inequivalent, which we show as  $H_{exo}$  and  $H_{endo}$  in Scheme 1. This notation

#### Scheme 1



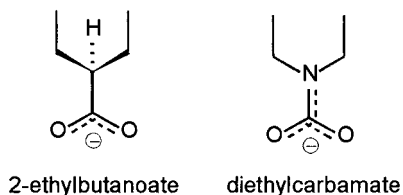
for the methylene protons was chosen to distinguish between those methylene protons pointing in toward the  $Mg_6$  cluster (*endo*) or outward toward the solution (*exo*). Symmetry considerations predict that **1** has twelve sets of magnetically distinct  $-CH_2-$  protons ( $H_{endo}$ ,  $H_{exo}$ ), six sets of  $-CH_3$  protons ( $H_\beta$ ), and twelve sets of carbon nuclei from the ethyl groups ( $C_\alpha$ ,  $C_\beta$ ). The 500 MHz 1D proton NMR spectrum in Figure 4 does not permit us to resolve all twelve  $H_{endo/exo}$  proton signals due to considerable overlap. However, the splitting patterns observed in the  $-CH_2-$  region, Figure 4 inset, can only be interpreted based on the inequivalence of  $H_{exo}$  and  $H_{endo}$  on the NMR time scale and indicates that  $C_\alpha$ –N bond rotation must be substan-

(11) Shannon, R. D. *Acta Crystallogr.* **1976**, A32, 751.



tially hindered. In the ethyl region between 2.6 and 4.1 ppm, the spectrum shows a well-defined manifold of signals, arising from  $H_{exo}$  and  $H_{endo}$ . This 1D manifold consists of a series of at least nine resolvable sextet signals. Each sextet signal has hyperfine intensities in the ratio 1:3:4:4:3:1, implying an  $ABX_3$  nuclear spin system for the ethyl groups in which A and B represent inequivalent  $H_{exo}$  and  $H_{endo}$  methylene protons and X represents three equivalent  $H_\beta$  protons of one ethyl group. Therefore, while  $C_\alpha-N$  rotation is hindered,  $C_\alpha-C_\beta$  rotation is rapid and averages all three methyl protons. The  $ABX_3$  coupling scheme gives rise to the observed 1:3:4:4:3:1 sextet if the proton-proton coupling constant  $J_{AB}$  is equal to  $2J_{AX}$ , as shown in Figure 4. Inspection of the 1D proton spectrum gives  $J_{AX} \approx$

#### Scheme 2



7 Hz for the  $H_{endo/exo}-H_\beta$  couplings and  $J_{AB} \approx 14$  Hz for the  $H_{endo}-H_{exo}$  couplings, which are essentially invariant within experimental error for all of the ethyl signals.

While the  $H_\beta$  and  $H_{endo/exo}$  resonances are highly overlapping in the 1D proton and  $^{13}C$  NMR spectrum, 2D  $^1H\{-^{13}C\}$  NMR correlation spectroscopic methods permitted resolution and nearly complete assignment of all of the  $^{13}C$  and  $^1H$  resonance frequencies which are summarized in Table S1.<sup>12</sup> Twelve  $^{13}C-^1H$  cross-peaks, corresponding to all of the expected single-bond  $C_\alpha-H_{endo/exo}$  couplings, are resolved in the methylene region of the HMQC spectrum, Figure S1.<sup>12</sup> The expected six couplings are observed in the methyl region (not shown). The HMBC method, which permits observation of two- and three-bond couplings, showed the expected couplings between  $C_\alpha$  and  $H_\beta$ . However, it also showed three-bond couplings from  $C_\alpha$  across the carbamate nitrogen atom to  $H_{endo'}$  and  $H_{exo'}$  on an inequivalent ethyl group, Figure S2,<sup>12</sup> permitting assignment of these signals to ligands B and C. Most importantly, we also observed  $C_\alpha-H_{endo/exo}$  couplings, which permitted correlation of  $H_{endo/exo}$  with the appropriate  $^{13}C_c$  signal from the 1D spectrum and complete assignment of the NMR spectrum based on the positions of each  $H_{endo/exo}$  proton in the structure, Figure S3.<sup>12</sup> HMBC and HMBC correlation data are presented in Table S2.<sup>12</sup> The only ambiguity in the correlated assignments in Table S1<sup>12</sup> is that we are unable to conclusively distinguish and assign ethyl groups B and B'.

The NMR frequencies of the  $H_{endo}$  and  $H_{exo}$  protons are consistent with different chemical environments. The  $H_{endo}$  protons pointing inward toward the  $Mg_6O_{12}$  cluster are in a more electronegative environment and are shifted downfield when compared to the  $H_{exo}$  protons which are pointing outward toward the bulk solvent. The  $H_{endo}$  protons of groups C, C', and D share closer contacts with neighboring O and N atoms than do groups A, B, and B' and therefore show a larger difference in chemical shifts between  $H_{endo}$  and  $H_{exo}$  protons.

#### Discussion

Helicity in simple coordination complexes arises from right-handed ( $\Delta$ ) and left-handed ( $\Lambda$ ) stereochemistry of octahedral or tetrahedral metal ions. The present paradigm for rational

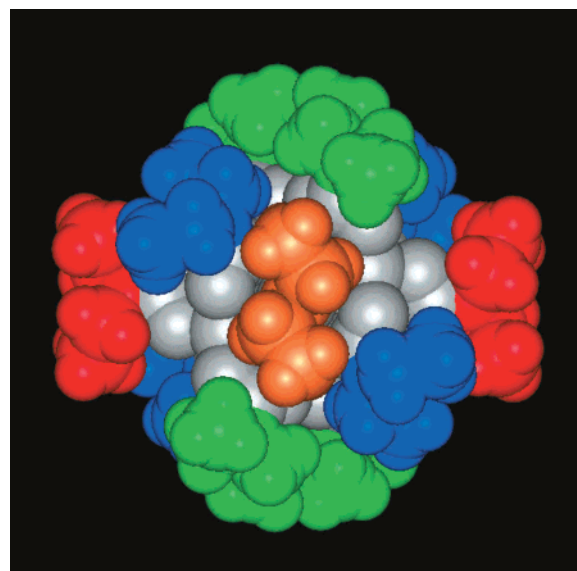


**Figure 5.** Space-filling model of **1** based on X-ray data and consistent with NMR spectrum. The  $Mg_6O_{24}$  core is shown in light gray. The ethyl groups are color-coded as follows: red = A, green = B, blue = C, orange = D.

design of multinuclear synthetic double and triple helices is predicated on the cross-linking of multidentate ligands with tetrahedral or octahedral metal ions,<sup>6</sup> exploiting the handedness of the metal ions' coordination sphere to impart the helical twist to the polymeric ligand.<sup>13</sup> Helicity in **1** arises from the fact that two facially disposed edges of the central six-coordinate  $Mg^{2+}$  ion are shared with terminal five-coordinate ions. If the five-coordinate ions are considered as bidentate ligands to the central six-coordinate ion, then we see that the helicity in each trinuclear  $Mg_3O_{12}$  chain also results from  $\Delta$  and  $\Lambda$  stereochemistry of the central pair of  $Mg^{2+}$  ions.

While the six-coordinate metal ions impart the helical twist to **1**, the ligands must play a critical role in governing the global topology of the complex. This idea is reinforced by the fact that despite the structural similarity between carbamate and carboxylate anions, there is no hexanuclear carboxylato analogue for the double helical  $Mg_6(Et_2NCO_2)_{12}$  complexes. One structural feature present in all carbamate complexes is the planar  $sp^2$  hybridized nitrogen atom of the carbamate ligand, which contrasts with the saturated tetrahedral  $C_\alpha$  carbon atom in carboxylate anions, Scheme 2. There are two important consequences for the carbamate anion. First, delocalization of the nitrogen lone pair onto the carbonyl carbon places additional negative charge on the carbamate oxygens, which can be dissipated through bridging interactions to multiple magnesium ions. For example, ligand D in Figure 2 bridges four different magnesium ions, a motif unprecedented in crystallographically characterized magnesium carboxylate complexes. This provides structural stability for cross-linking two magnesium trimers to give the hexanuclear magnesium cluster. Second, the planar nitrogen provides a more symmetric disposition of the pendant alkyl groups in diethylcarbamate compared to the analogous 2-ethylbutanoate anion, which has a tetrahedral carbon in the  $\beta$ -position. This permits more efficient packing of the ethyl groups around the magnesium cluster in **1**, which would be disrupted if a nonplanar ligand were substituted. A space-filling model of **1**, Figure 5, demonstrates that the ethyl groups pack very efficiently around the core and interlock like the pieces of

(12) Deposited in supplementary information.

(13) Pierre, J.-L. *Coord. Chem. Rev.* **1998**, 178–180, 1183–1192.

a puzzle so that rotation around the  $C_{\alpha}$ -N bond is hindered by steric contacts with one or more other ethyl groups. As a consequence, the ethyl groups form a hydrophobic secondary solvation shell providing only limited access to the hydrophilic  $Mg_6O_{24}$  core. The stability of this organic sheath is reinforced by hindrance to  $C_c$ -N bond rotation resulting from partial double bond character in the  $C_c$ -N bond. These two factors combine to provide a hydrophilic core surrounded by a hydrophobic shell of considerable conformational stability as shown by the sharp solution NMR spectra.

The overall shape of the molecule is oblate, with dimensions on the nanometer scale (approximately  $10 \text{ \AA} \times 15 \text{ \AA} \times 16 \text{ \AA}$ ). Because only the organic sheaths are exposed to each other in the solid state, crystal interactions will be dominated by weak van der Waals forces, leading to a simple crystal packing structure. Another consequence of the inverted-micelle-like structure of **1** is its high solubility in hydrocarbons and other very nonpolar solvents. Preliminary studies indicate that one or more of the magnesium ions in **1** can be replaced with divalent transition metal ions in a stepwise manner, indicating that **1** could be applied to the controlled dissolution of paramagnetic metal ions in very nonpolar media.

### Summary

We have extended the range of  $M_6(Et_2NCO_2)_{12}$  complexes to include the diamagnetic magnesium(II) ion, which permitted us to characterize its solution structure by NMR. The preparation

of **1** is an excellent example of the self-assembly concept, which leads in this case to a double helical complex prepared from simple nonpolymeric starting materials. The  $M_6(Et_2NCO_2)_{12}$  structure type in the solid state and solution appears to be confined to carbamate ligands, implying electronic and structural factors unique to the carbamate ligand. This suggests that the chemistry of carbamate complexes cannot always be extrapolated from carboxylate chemistry and that considerable work remains to fully elucidate their structural chemistry.

**Acknowledgment.** We acknowledge Jason Benedict for assistance in reproduction of the syntheses of **1**. Dr. Mike Williams assisted in obtaining the 2D NMR data. Financial support for this work was provided by the National Science Foundation (CHE 9985266 to M.T.C. and CHE 9808678 for upgrades to the NMR facility) and by the donors of the Petroleum Research Fund administered by the American Chemical Society.

**Supporting Information Available:** Table S1 ( $^1H$  and  $^{13}C$  NMR assignments for **1** based on 1D and 2D NMR), Table S2 (listing of HMQC and HMBC  $^{13}C$ - $^1H$  correlation data), Figure S1 (2D  $^1H$ - $\{^{13}C\}$  HMQC spectrum of **1** in the methylene region), Figure S2 (2D  $^1H$ - $\{^{13}C\}$  HMBC data for **1**), Figure S3 (diagram of **1** showing positions of  $H_{endo}$  and  $H_{exo}$  protons), and an X-ray crystallographic file in CIF format for the structure determination of **1**. These materials are available free of charge via the Internet at <http://pubs.acs.org>.

IC0009425